JYX
JYVÄSKYLÄN YLIOPISTO
UNIVERSITY OF JYVÄSKYLÄ

This is a self-archived version of an original article. This version may differ from the original in pagination and typographic details.

Author(s): Domínguez-Flores, Fabiola; Melander, Marko M.

Title: Approximating constant potential DFT with canonical DFT and electrostatic corrections

Year: 2023

Version: Published version

Copyright: © 2023 Author(s). Published under an exclusive license by AIP Publishing.

Rights: In Copyright

Rights url: http://rightsstatements.org/page/InC/1.0/?language=en

Please cite the original version:

Domínguez-Flores, F., & Melander, M. M. (2023). Approximating constant potential DFT with canonical DFT and electrostatic corrections. Journal of Chemical Physics, 158(14), Article 144701. https://doi.org/10.1063/5.0138197

The Journal of Chemical Physics

RESEARCH ARTICLE | APRIL 10 2023

Approximating constant potential DFT with canonical DFT and electrostatic corrections

Special Collection: Chemical Physics of Electrochemical Energy Materials

Fabiola Domínguez-Flores ; Marko M. Melander

Check for updates

J. Chem. Phys. 158, 144701 (2023)
https://doi.org/10.1063/5.0138197

View Online
Export Citation
CrossMark

30 June 2023 07:06:11

AIP Publishing

The Journal of Chemical Physics
Special Topic: Adhesion and Friction
Submit Today!
AIP Publishing

The Journal of Chemical Physics ARTICLE scitation.org/journal/jcp

Approximating constant potential DFT with canonical DFT and electrostatic corrections

Cite as: J. Chem. Phys. 158, 144701 (2023); doi: 10.1063/5.0138197
Submitted: 9 December 2022 • Accepted: 15 March 2023 •
Published Online: 10 April 2023

View Online Export Citation CrossMark

Fabiola Domínguez-Flores and Marko M. Melander[a)]

AFFILIATIONS

Department of Chemistry, Nanoscience Center, University of Jyväskylä, FI-40014 Jyväskylä, Finland

Note: This paper is part of the JCP Special Topic on Chemical Physics of Electrochemical Energy Materials.
[a)]**Author to whom correspondence should be addressed:** marko.m.melander@jyu.fi

ABSTRACT

The complexity of electrochemical interfaces has led to the development of several approximate density functional theory (DFT)-based schemes to study reaction thermodynamics and kinetics as a function of electrode potential. While fixed electrode potential conditions can be simulated with grand canonical ensemble DFT (GCE-DFT), various electrostatic corrections on canonical, constant charge DFT are often applied instead. In this work, we present a systematic derivation and analysis of the different electrostatic corrections on canonical DFT to understand their physical validity, implicit assumptions, and scope of applicability. Our work highlights the need to carefully address the suitability of a given model for the problem under study, especially if physical or chemical insight in addition to reaction energetics is sought. In particular, we analytically show that the different corrections cannot differentiate between electrostatic interactions and covalent or charge-transfer interactions. By numerically testing different models for CO_2 adsorption on a single-atom catalyst as a function of the electrode potential, we further show that computed capacitances, dipole moments, and the obtained physical insight depend sensitively on the chosen approximation. These features limit the scope, generality, and physical insight of these corrective schemes despite their proven practicality for specific systems and energetics. Finally, we suggest guidelines for choosing different electrostatic corrections and propose the use of conceptual DFT to develop more general approximations for electrochemical interfaces and reactions using canonical DFT.

Published under an exclusive license by AIP Publishing. https://doi.org/10.1063/5.0138197

30 June 2023 07:06:11

I. INTRODUCTION

Evaluation of electrocatalytic thermodynamics and kinetics with density functional theoretical methods has received significant interest during the past 20 years.[1] Early on, Lozovoi *et al.* noted that electrochemical interfaces cannot be properly treated with constant charge (canonical) density functional theory (DFT) calculations because the experimentally relevant constant potential measurements correspond to the grand canonical ensemble (GCE).[2] Lozovoi *et al.* also showed that canonical DFT calculations correspond to a capacitor or an STM device rather than an electrochemical interface.[2] Furthermore, during the last 5 years, it has been theoretically shown that the GCE-DFT[3] provides, in principle, an exact description of electrochemical and electrocatalytic thermodynamics and kinetics.[4–6] GCE-DFT naturally captures the charge fluctuations[7] needed to maintain a constant electrode potential and can at least, in principle, account for the rapid charge injection during an electrochemical reaction.[8] The development of practical GCE-DFT methods has led to the situation where it is now technically possible to simulate both kinetics and thermodynamics directly with GCE-DFT.[9,10]

In addition to direct GCE-DFT simulations, several electrostatic schemes have been developed to enable the application of canonical, constant charge DFT to approximate GCE-DFT.[11–25] In practice, the developed electrostatic approximations work rather well for predicting reaction energetics. However, different schemes have been applied to different systems and it is not *a priori* clear which scheme would be most appropriate for a given system. At a more fundamental level, it remains unclear how well these different models actually capture the chemistry and physics of electrochemical interfaces or electrocatalysis. For instance, all electrostatic corrections are based on the separation of chemical and electrostatic interactions such that potential-dependent or "electrochemical" contributions are computed with electrostatic schemes akin to the classical Frumkin correction.[26] The Frumkin correction should, however, be applied to outer-sphere electron transfer reactions

Published under an exclusive license by AIP Publishing

only,[26] but the electrostatic DFT schemes are primarily used for studying electrocatalytic inner-sphere reactions without formal justification. Furthermore, all electrostatic approximations can be systematically developed by treating the electrochemical interface as a capacitor (*vide infra*). Hence, the electrostatic corrections seem to contradict Lozovoi's conclusions, raising the question if and when electrochemical interfaces can be treated as capacitors.

To understand how well different electrostatic corrections on canonical DFT capture the physics and chemistry of electrochemical interfaces, we systematically derive and analyze various previously developed and widely used approaches such as capacitor, multi-capacitor, and dipole field models. We use different approaches and methods from conceptual DFT, classical electrostatics, GCE-DFT, canonical DFT, and thermodynamics to analyze which implicit assumptions are included in different electrostatic corrections and how these might impact their robustness, convergence, and physical insight. In agreement with previous studies, we arrive to the conclusion that various electrostatic corrections on top of canonical DFT calculations can reliably reproduce or fit reaction energies at different electrode potentials. However, our analysis highlights the implicit assumptions behind these different approximations and that physical insight from such fits is limited and depends heavily on the chosen scheme. After analyzing the limitations of different approximations, we provide guidelines for choosing an appropriate electrostatic method for a given system. We also propose beyond-electrostatic corrections to include charge transfer concepts and covalent bonding effects in an effective manner using conceptual DFT. Overall, we show that while electrostatic corrections to canonical DFT can be used to fit electrochemical thermodynamics, the electrostatic scheme needs to be chosen with care and validated case by case if some physical or chemical insight is sought.

II. RESULTS

In computational electrochemistry and electrocatalysis, DFT is most often used for computing (free) energy differences related to adsorption, reaction thermodynamics, or kinetics. We will focus on how the electrochemical conditions, i.e., the electrolyte and the electrode potential, influence these energetic differences. Different electrostatic approximations attempt to model potential-dependent reaction (free) energies ($\Delta E(U)$) using corrections ($dE(U)$) on reference state ($\Delta E(ref)$) energetics using a generic expression,

$$\Delta E(U) = \Delta E(ref) + dE(U), \tag{1}$$

where U is the electrode potential. We study different approximations to the potential-dependent *differential free energies* $dE(U)$ both in the grand canonical ($d\Omega$) and Helmholtz (dA) ensembles.

Below, we first present the general formulation of integral and differential free energies in the grand canonical and canonical ensembles. We then assume that geometric changes are suppressed and that chemical and electrostatic interactions can be separated. These are common approximations to all electrostatic approximations, which allow us to derive and focus on various previously developed corrections such as the capacitor, multi-/partitioned capacitor, and dipole field approximations. This is followed by the analysis of geometric changes as a function of the potential and the general validity of separating electrostatic interactions from charge transfer effects and covalent bonds (Table I). Different approximations are tested for the CO_2 electrosorption step on a prototypical single-atom iron–nitrogen graphene Fe–NC catalyst.

A. GCE-DFT

GCE-DFT describes the thermodynamic state of an electrochemical system under constant temperature (T), volume (V), and (electro)chemical potential ($\{\tilde{\mu}_i\}$) conditions, as shown in Fig. 1. The electrochemical potential of electrons within the electrode ($\{\tilde{\mu}_n\}$) is equal to the absolute electrode potential.[27] The constant electrode potential condition is enforced by fixing the electrochemical potential of electrons in the electrode ($\tilde{\mu}_n$), whereas constant electrolyte activity is set by fixing the electrolyte chemical potential ($\tilde{\mu}_\pm$).[5] The equilibrium GCE free energy, Ω, in turn, is a functional of the nuclear/electronic GCE density operator ($\hat{\rho}_\mu$): $\Omega[\hat{\rho}_\mu](T, V, \{\tilde{\mu}_i\})$,

TABLE I. Summary of the various approximations derived in this work.

A Eq. (6)	Free energy in the Helmholtz ensemble
A_{el} Eq. (9)	Linear electrochemical free energy correction
$A_{el,cap}$ Eq. (13)	Electrostatic free energy form from a capacitor
A_{cap} Eq. (14)	Free energy form from a capacitor
$A_{cap,\,part}$ Eq. (17)	Free energy form of the multicapacitor approximation
$A_{cap,\,series}$ Eq. (18)	Free energy form from a capacitive system in series
$A_{cap,\,parallel}$ Eq. (19)	Free energy from a capacitive system in parallel
$A_{cap,\,part,\,mixed}$ Eq. (21)	Free energy from mixing parallel and series partitions
$A_{cap,\,part,\,average}$ Eq. (22)	Free energy form of the capacitor partition with an average number of electrons
$A_{charge,\,field}$ Eq. (24)	Free energy form of the electron potential in function of the surface charge
A_{es} Eq. (27)	Free energy form of the multipole expansion
$A_{dip-field}$ Eq. (32)	Free energy form of the field-dependent model
$A_{eff.dip-field}$ Eq. (33)	Free energy form of the effective dipole model
$A_{dip-geom}$ Eq. (34)	Free energy form of the energetics of the electrode potential-driven changes in the geometry

30 June 2023 07:06:11

Published under an exclusive license by AIP Publishing

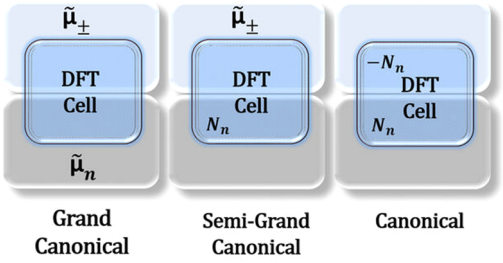

FIG. 1. Schematic representation of the different thermodynamic ensembles.

$$\Omega[\hat{\rho}_{\mu}](T,V,\{\tilde{\mu}_i\}) = A(N_i;\{\tilde{\mu}_i\}) - \sum_i \tilde{\mu}_i N_i, \tag{2}$$

where N_i is the expectation value for the number of species i and $A(N_i;\{\tilde{\mu}_i\})$ is the canonical free energy at a constant electrode potential. Ω includes all quantum effects for electrons and nuclei at thermodynamic equilibrium, and is, in principle, exact by construction.[5] $\Omega[\hat{\rho}_{\mu}](T,V,\{\tilde{\mu}_i\})$ also shows that the grand canonical free energy depends explicitly on the chemical potentials of all components in the system. This indicates that all chemical potentials and, hence, concentrations can be controlled independently: one can change the electrode potential without impacting electrolyte activity.

For the computation of reaction thermodynamics and kinetics, it is also useful to define grand free energy differentials. This can be done in the framework of GCE conceptual DFT.[28–30] We assume that the temperature and volume are fixed, in which case the differential grand canonical energy is[30]

$$d\Omega = \sum_{i\in n,\pm}\left(\frac{\partial\Omega}{\partial\tilde{\mu}_i}\right)_{v(\mathbf{r}),\tilde{\mu}_{i\neq j}} d\tilde{\mu}_i + \int\left(\frac{\delta\Omega}{\delta v(\mathbf{r})}\right)_{\{\tilde{\mu}_i\}}\delta v(\mathbf{r})d\mathbf{r}, \tag{3}$$

where $v(\mathbf{r})$ is the external potential due to the nuclei. The reaction pathways under constant (electro)chemical potentials can then be mapped by varying $v(\mathbf{r})$ to present nuclear movement. Variations in the electrode potential and the result of the electrostatics are encoded in $\tilde{\mu}_i$ since they depend on the average electrostatic potential $\langle\phi^E(\mathbf{r})\rangle$ as[27,31]

$$\tilde{\mu}_i^P = \mu_i^{0,M} + z_i\langle\phi^P(\mathbf{r})\rangle, \tag{4}$$

where z is the charge of species i in phase P and eV units are used. Within the electrode, $\phi^E = \langle\phi^E(\mathbf{r})\rangle$ is equal to the electrode inner potential, which uniquely defines the electrode potential.[27,31] The first term in Eq. (3) can then be written as a function of the electrode potential U,

$$\left(\frac{\partial\Omega}{\partial\tilde{\mu}_n}\right)_{v(\mathbf{r}),\tilde{\mu}_{\pm}} = -\left(\frac{\partial\Omega}{\partial\phi^E}\right)_{v(\mathbf{r}),\tilde{\mu}_{\pm}} = -\left(\frac{\partial\Omega}{\partial U}\right)_{v(\mathbf{r}),\tilde{\mu}_{\pm}}, \tag{5}$$

which shows that the electrostatic potential within the electrode, i.e., the inner potential, defines the relationship between the grand free energy and electrostatics. As the inner potential is determined by the electrode charge density through the Coulomb potential [Eq. (26)], the relationship between charge (density), electrostatics, and free energy is established. In practical GCE-DFT calculations, the Hartree potential is used as a proxy for the inner potential and only its changes are meaningful and unique.[32]

B. Canonical DFT, computational hydrogen electrode, and Frumkin and capacitor corrections

Constant charge or canonical DFT describes the thermodynamics in the Helmholtz ensemble where the number of particles (N_i), T, and V are fixed. The relevant energy functional A is written in terms of the thermal density operator $\hat{\rho}_T$: $A[\hat{\rho}_T(T,V,\{N_i\})]$. This functional is, in principle, exact but does not correspond to constant electrode potential or constant electrolyte activity conditions. At constant volume and temperature, the canonical free energy differential is[28]

$$dA = \sum_{i\in n,\pm}\left(\frac{\partial A}{\partial N_i}\right)_{v(\mathbf{r}),N_{i\neq j}} dN_i + \int\left(\frac{\delta A}{\delta v(\mathbf{r})}\right)_{\{N_i\}}\delta v(\mathbf{r})d\mathbf{r}. \tag{6}$$

Unlike in GCE-DFT, the canonical free energy and the number of electrons do not explicitly depend on the electrode potential (see Fig. 1). Furthermore, in practical canonical DFT calculations, the number of electrons and electrolyte concentration cannot be independently controlled since charge neutrality needs to be maintained. This shows the first flaw of canonical DFT calculations for electrochemical systems: in simulations, the number of electrons and electrolyte concentration (or number of ions) are not truly independent variables as they are in experiments. In principle, this can be easily fixed by performing the calculations in a semi-grand canonical ensemble where the electrolyte chemical potential $(\tilde{\mu}_{\pm})$ rather than the number of ions is fixed, as shown in Fig. 1.

To study the impact of the electrode potential, canonical DFT simulations control the number of electrons or the surface charge, which are connected to the electrode potential through the self-consistently computed Fermi level, E_F, which itself is a function of both $v(\mathbf{r})$ and $\{N_i\}$. Changes in the Fermi level are in turn directly proportional to both electrode potential and inner-potential differences: $\Delta U = -\Delta E_F = -\Delta\tilde{\mu}_e = \Delta\phi^E$. For the sake of clarity, we consider electrode dependency within the semi-grand canonical ensemble with fixed $\tilde{\mu}_{\pm}$. In this case, the electron electrochemical potential is

$$\begin{aligned}\tilde{\mu}_n = \left(\frac{\partial A}{\partial N_n}\right)_{v(\mathbf{r}),\tilde{\mu}_{\pm}} &= \left(\frac{\partial A}{\partial U}\right)_{v(\mathbf{r}),\tilde{\mu}_{\pm}}\left(\frac{\partial U}{\partial N_n}\right)_{v(\mathbf{r}),\tilde{\mu}_{\pm}} \\ &= -\frac{\left(\frac{\partial A}{\partial U}\right)_{v(\mathbf{r}),\tilde{\mu}_{\pm}}}{C(U)} \approx -\frac{\left(\frac{\partial A}{\partial U}\right)_{v(\mathbf{r}),\tilde{\mu}_{\pm}}}{C_{eff}},\end{aligned} \tag{7}$$

where the minus sign on the second row comes from the definition of the capacitance with respect to the number of electrons or surface charge (σ): $C(U) = \frac{\partial\sigma}{\partial U} = -\frac{\partial N_n}{\partial U}$. The potential-dependent $(C(U))$ and *constant* effective (C_{eff}) differential capacitances were also introduced,

$$\begin{aligned}\left(\frac{\partial^2 A}{\partial N_n^2}\right)_{v(\mathbf{r}),\tilde{\mu}_{\pm}} &= \left(\frac{\partial\tilde{\mu}_n(N_n)}{\partial N_n}\right)_{v(\mathbf{r}),\tilde{\mu}_{\pm}} = -\left(\frac{\partial U_n(N_n)}{\partial N_n}\right)_{v(\mathbf{r}),\tilde{\mu}_{\pm}} \\ &= \frac{1}{C(U)} \approx \frac{1}{C_{eff}}.\end{aligned} \tag{8}$$

30 June 2023 07:06:11

Published under an exclusive license by AIP Publishing

This equation shows that modeling the Helmholtz free energy as a function of the electrode potential requires reliable estimates for either the partial derivatives or the effective capacitance.

The simplest electrochemical approximation to $A(U)$ is obtained by assuming that all potential-dependency is captured through the electrostatic potential. In this case, one obtains the linear electrochemical free energy correction $A_{el}(N_n) \approx A(N_{n0}) - (N_n - N_{n0})\phi^E = A(N_{n0}) - \Delta N_n \phi^E$ around a reference free energy with N_{n0} electrons for a reaction where ΔN_n electrons are transferred. Equation (7) then gives

$$\left(\frac{\partial A_{el}}{\partial N_n}\right) \approx -\frac{\frac{\partial A(N_{n0})-\Delta N_n\phi^E}{\partial U}}{C_{eff}} = -\frac{\frac{\partial A(N_{n0})}{\partial U} - \Delta N_n}{C_{eff}}$$
$$\rightarrow \frac{\partial A(N_{n0})}{\partial U} = -\left(C_{eff}\frac{\partial A_{el}}{\partial N_n} + \Delta N_n\right), \tag{9}$$

where it is implied that $\nu(\mathbf{r})$, $\tilde{\mu}_\pm$, and ΔN_n are kept fixed. This equation provides a relation between the canonical free energy, electrode potential, and number of electrons assuming effective constant capacitance. Assuming that $\frac{\partial A(N_n)}{\partial N_n} = 0$ reduces Eq. (10) to $dA_{el} \approx -\frac{\partial \phi}{\partial N_n} dN_n = \frac{dN_n}{C_{eff}}$, which is a simple capacitive correction developed, e.g., in Ref. 21. Alternatively, one can assume that the canonical energy of A_{el} does not explicitly depend on the number of electrons in the system $\left(\frac{\partial A(N_{n0})}{\partial U} = 0\right)$ in which case Eq. (10) provides a purely electrostatic correction, and Eq. (9) leads to a linear, Nernstian relation between the electrode potential and free energy. If the same assumption is made for proton-coupled electron transfer (PCET) thermodynamics, Eq. (9) would be equivalent to the computational hydrogen electrode (CHE) method,[33] which also predicts that PCET reactions exhibit Nernstian behavior against the electrode potential.

To go beyond linear Nernstian or CHE behavior, a general capacitance relation for $\partial A_{el}/\partial N_n$ or $\partial A/\partial U$ is needed. Various approximations have been developed to the differential $\partial A/\partial U$, but to mention one, the significant work[25] of Hörmann *et al.* shows how this term can be efficiently computed as a first-order correction to the CHE or Nernstian models. In the crudest approximation, the Helmholtz free energy depends linearly on the electrode potential and $dA_{el} = (\partial A_{el}/\partial N_n)dN_n$, which is valid when $dT = dV = 0$. Including the differential capacitance as $C = -\partial N_n/\partial U$, one obtains

$$dA_{el} \approx -\frac{\frac{\partial A_{el}(N_n)}{\partial U}}{\frac{\partial N_n}{\partial U}} \times dN_n = -\frac{\partial A_{el}(N_n)}{\partial N_n} \times dN_n = -\tilde{\mu}_n(N_n)dN_n, \tag{10}$$

which shows that the free energy dA_{el} contains both an electrostatic and chemical term, and depends linearly on the number of electrons around some electrochemical potential $\tilde{\mu}_n$. This form closely resembles the Frumkin correction as can be seen by noticing that the electrochemical potential in different phases is equal in equilibrium. This allows one to replace the electrode potential $(\tilde{\mu}_n)$ with the corresponding electron electrochemical potential of the solvent phase $(S, \tilde{\mu}_n^S)$. Combining Eq. (10) and Eq. (4) for $\tilde{\mu}_n^S$ yields an expression practically equal to the Frumkin correction: $dA_{Frumkin}(\mathbf{r}) \propto \phi^S(\mathbf{r})dN_n$ with the electrostatic potential $\phi^S(\mathbf{r})$ in the reaction plane corresponding to $\tilde{\mu}_n$.

To describe non-linear effects in the free energy, Eq. (9) can also be written in terms of the electrode potential and number of electrons without the effective capacitance,

$$\left(\frac{\partial A_{el}}{\partial N_{n0}}\right)_{\nu(\mathbf{r}),\tilde{\mu}_\pm} \approx \frac{\frac{\partial A_{el}(N_{n0})-\Delta N_n\phi^E}{\partial U}}{\partial N_{n0}/\partial U}$$
$$= \left(\frac{\partial A_{el}(N_{n0})}{\partial N_{n0}} - \Delta N_n \frac{\partial U}{\partial N_{n0}}\right)$$
$$\rightarrow dA_{el} \approx \left(\frac{\partial A_{el}(N_{n0})}{\partial N_{n0}} - \Delta N_n \frac{\partial U}{\partial N_{n0}}\right)dN_{n0}, \tag{11}$$

where ΔN_n is fixed. A physically appealing approximation to $\partial A_{el}/\partial N_{n0}$ can be developed by considering a situation where the electrode and electrolyte are successively charged (a capacitor). Consider that the charge (density) of the electrode is changed from $N_{n0} = \int_{V_{electrode}} d\mathbf{r}\rho_{n0}(\mathbf{r})$ to $N_{n1} = \int_{V_{electrode}} d\mathbf{r}\rho_{n1}(\mathbf{r})$. To maintain charge neutrality, the electrolyte charge density also changes from $-N_{n0} = \int_{V_{electrolyte}} \rho_{\pm,0}(\mathbf{r})$ to $-N_{n1}$. As the electrode and electrolyte are physically distinct phases, their volumes do not overlap. Such a division can be achieved on a macroscopic scale using, e.g., the Gibbs dividing surface but is very difficult to achieve at the molecular level where the division between the electrode and electrolyte or solvent regions is not well-defined. If we assume that such a separation can be achieved and that the electrolyte volume and all interactions apart from electrostatics remain unchanged, the electrostatic work to assemble a charge state for phase i is

$$W_{el}^i = \frac{1}{2}\iint d\mathbf{r}d\mathbf{r}'\frac{\rho_{n,i}(\mathbf{r})\rho_{\pm,i}(\mathbf{r})}{|\mathbf{r}-\mathbf{r}'|} = \frac{1}{2}\int d\mathbf{r}\rho_{\pm,1}(\mathbf{r})\phi_e(\mathbf{r}), \tag{12}$$

which provides the electrostatic interaction energy between the electrolyte charge density and the electrostatic potential ϕ_e generated by the electrode [see Eq. (26)]. For two conductors, here the electrode and electrolyte, the electrostatic work is equal to that of a single capacitor: $W_{cap}^i = \frac{N_{n,i}N_{\pm,i}}{2C_{eff}} = \frac{N_n^2}{2C_{eff}}$. When temperature and volume are kept constant, the differential free energy is the electric work done on the system, and Eq. (11) becomes

$$dA_{el,cap} \approx \left(\frac{\partial W_{cap}}{\partial N_{n0}} - \frac{\partial U}{\partial N_{n0}}\right)dN_{n0} = \left(\frac{N_{n0}}{C_{eff}} + \frac{1}{C_{eff}}\right)dN_{n0}$$
$$\rightarrow A_{el,cap} = W_{cap} + N_{n0}/C_{eff}. \tag{13}$$

This equation is essentially the capacitative correction developed in Ref. 21, and the only difference is the constant N_{n0} term, which arises from our choice of using electrochemical [see Eq. (9)] rather than chemical potentials to carry out the analysis. The above-mentioned developments exemplify the physical basis and main approximations in the capacitor models that are treated more systematically in subsequent sections.

C. The capacitor approximation

The systematic development of capacitor-based schemes is achieved through the Taylor expansion of the Helmholtz energy with respect to the number of electrons rather than assuming effective forms for the electrostatic interactions—the physical basis, however, is the same. The Taylor expansion perspective is very

30 June 2023 07:06:11

Published under an exclusive license by AIP Publishing

general but will always rely on the tacit assumption that an electrochemical interface can be treated as a mere double-layer capacitor and that all electrochemical reactions are just pseudo-capacitive processes.[22] The supplementary material, Secs S1–S2, shows that the Taylor expansion of canonical and grand canonical free energies is equally valid and share the same approximations. However, other derived thermodynamic quantities such as pressure and surface tension are thermodynamically consistent only in the GCE.[34]

The capacitor approximations result from a second-order Taylor expansion of the canonical free energy with respect to the number of electrons in the system. This is not only mathematically convenient but also physically motivated as it captures potential-dependency through (surface) charge and constant effective capacitance from Eq. (8). As shown in detail in the supplementary material, the second-order approximation is

$$A(N_n)_{cap} \approx A(N_{n0}) + \tilde{\mu}_n(N_{n0})dN_n + \frac{(dN_n)^2}{2C_{eff}(N_{n0})} + \mathcal{O}(dN^3) \quad (14)$$

around the reference system with N_{n0} electrons.

In the previous equation, the electrolyte properties cannot be controlled independently of surface charges since charge neutrality needs to be maintained. This problem can, however, be fixed by switching to a semi-grand canonical ensemble (see Fig. 1) where the electrolyte chemical potentials are constant, and the previous equation can be generalized to

$$A(N_n, \tilde{\mu}_\pm)_{cap} \approx A(N_{n0}) + \left(\frac{\partial A}{\partial N_n}\right)_{\nu(\mathbf{r}),\tilde{\mu}_\pm} dN_n + \frac{(dN_n)^2}{2}\left(\frac{\partial^2 A}{\partial N_n^2}\right)_{\nu(\mathbf{r}),\tilde{\mu}_\pm}, \quad (15)$$

where the constant electrolyte chemical potential and external potential are implied. In practice, the constant $\tilde{\mu}_\pm$ condition can be fulfilled by using any Poisson–Boltzmann model variant combined with the Lagrange multiplier technique to enforce charge neutrality.[5,35] Choosing the reference state N_{n0} to correspond to the potential of zero free charge (PZC), a convenient form for the differential Helmholtz energy within the capacitor approximation is obtained,

$$dA(N_n)_{cap} = \frac{\partial A_{cap}}{\partial N_n} dN_n \approx \left(\tilde{\mu}_n(N_{n0}) + \frac{dN_n}{C_{eff}(N_{n0})}\right) dN_n, \quad (16)$$

where the constant electrolyte chemical and external potentials are again implied. The linear term captures the Nernstian CHE-like behavior, while the quadratic term is the capacitive correction. Note that an equivalent expression is obtained by performing the Taylor expansion and subsequent steps in terms of the number of electrolyte ions rather than electrons: this implies that the capacitor model cannot reliably distinguish electrode potential from electrolyte-induced changes in the Helmholtz energy. This was also noted in Ref. 17 where it was shown that the same electrode potential can be obtained at different (surface) charges depending on the description of the solvent or electrolyte.

Both the fully canonical and semi-grand canonical variants of the capacitor model can be expressed in terms of the electron electrochemical potential and constant C_{eff}. While the constant capacitance approximation is common to all capacitor approximations, Eq. (8) shows that the effective capacitance depends not only on the electrode potential through the electron chemical potential but also on the electrolyte and the nuclear positions through $\nu(\mathbf{r})$. It is also well-known that capacitance does substantially depend on the adsorbates[36] and C_{eff} can even become negative due to chemisorption-induced changes in the surface dipole.[37] Some consequences of the constant capacitance approximation are addressed and discussed in more detail in Sec. II H.

The quality of the constant capacitance approximation naturally depends on the capacitance used to convert charge-dependent adsorption energies to potential-dependent energies as discussed in detail in the supplementary material, Sec. S2. The results therein show that potential-dependent differential adsorption energy relationships depend very sensitively on the capacitance used for converting charge variations to changes in the electrode potential. These results highlight that the effective capacitance must be self-consistently computed and not taken as a parameter from experiments or treated as a free parameter. Even if reasonable capacitance values are used, the differential adsorption energy from the capacitance is also symmetric with respect to the PZC. Such behavior is not observed in direct simulations of electrosorption energies. This will be discussed in more detail in Sec. II H.

D. The multicapacitor and partitioned capacitor approximations

In multicapacitor schemes, the total capacitance is broken down either into spatial contributions corresponding to electrode and electrolyte charging processes or to charge-transfer events due to adsorption, while reactions are treated as pseudo-capacitive events. Compared to the aforementioned original capacitor models, the multicapacitor models implicitly assume that the total charge or number of electrons in the system can be partitioned to non-interacting subsystems such as the electrode and reactants/adsorbate, explicit and implicit solvent volumes, or different regions of the electrode.[17,38] The general form of the multicapacitor energy expression is obtained by writing Eq. (15) as

$$A(N_n)_{cap,part} \approx A(N_n) + d(N_{n,r} + N_{n,e})\left(\frac{\partial A}{\partial N_n}\right)_{\nu(\mathbf{r})} + \frac{d(N_{n,r} + N_{n,e})^2}{2}\left(\frac{\partial^2 A}{\partial N_n^2}\right)_{\nu(\mathbf{r})}, \quad (17)$$

where N_n is the total number of electrons, $N_{n,r}$ is the number of electrons on the reactant, and N_e is the electrode charge. It must be noted that this Taylor expansion is well-defined only when *both* $N_{n,r}$ and $N_{n,e}$ are included in Eq. (17), but the resulting equation would be equal to the general capacitor model in Eq. (15). This indicates that the capacitance cannot be exactly separated to different contributions and that some approximations are always needed.

Different multicapacitor models are obtained by expressing the $\left(\frac{\partial^2 A}{\partial N_n^2}\right)_{\nu(\mathbf{r})}$ term in various ways. A physically motivated decomposition divides the total effective capacitance into multiple

30 June 2023 07:06:11

Published under an exclusive license by AIP Publishing

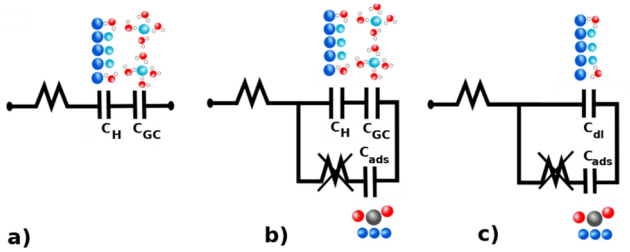

FIG. 2. Different equivalent circuits discussed in the text. (a) The serial Gouy–Chapman model consisting of double-layer (DL) and Helmholtz (H) capacitances. (b) Frumkin–Melik–Gaikazyan model shows a circuit including adsorption (ads) capacitance in parallel with the Gouy–Chapman and Helmholtz capacitances. (c) The Grahame model with adsorption and DL capacitances. The resistances are neglected in the thermodynamic treatment.

capacitors either in series or parallel. The serial situation corresponds to non-interacting capacitors where each capacitor has its own energy and the total capacitor energy is the sum of the individual i capacitors with potential V: $E_{cap,series} = \sum_i W_{i,cap} = \frac{N^2}{2C_{eff}} = \sum_i \frac{N_i^2}{2C_{i,eff}}$. For the series case, there is only one effective capacitance, which cannot be easily separated: $E_{cap,series} = \frac{N^2}{2C_{eff}} = \frac{N^2}{2\sum_i C_i}$. Figure 2 shows that the serial and parallel connections correspond to distinct physical and chemical processes at the electrochemical interface. This fact is widely used in electrochemical impedance spectroscopy where different equivalent circuits are applied to interpret the total capacitance in terms of adsorption, double-layer, and other charge-transfer processes.[39,40] The equivalent circuit in Fig. 2(a) shows how the total effective capacitance can be separated as diffuse, Gouy–Chapman and compact, Helmholtz contributions using capacitors in series ($1/C_{DL} = 1/C_{GC} + 1/C_H$). Figure 2(c) shows the Grahame model that treats capacitors in parallel to model the double-layer capacitance and charge transfer or specific adsorption as pseudo-capacitive ($C_{eff} = C_{ads} + C_{DL}$). The extended Grahame or Frumkin–Melik–Gaikazyan[41] circuit shown in Fig. 2(b) further decomposes the double-layer capacitance to Gouy–Chapman and Helmholtz contributions.

The choice of an appropriate equivalent circuit model is crucial for rationalizing and understanding electrochemical reactions within the multicapacitor approximations. As most DFT studies address electrochemical adsorption processes and surface reaction steps, the (extended) Grahame or Frumkin–Melik–Gaikazyan model of parallel capacitors would be the most relevant equivalent circuit. This is, however, not the model adopted in partitioned or multicapacitor approaches because the total capacitance cannot be partitioned without further approximations. Rather than using the Grahame model, current multicapacitor approaches use either serial or parallel capacitors, and estimate the Helmholtz free energy as

$$A(N_n)_{cap,series} = A(N_n) + d(N_{n,r} + N_{n,e})\left(\frac{\partial A}{\partial N_n}\right)_{v(\mathbf{r})} + \frac{d(N_{n,r} + N_{n,e})^2}{2}\left(\frac{1}{C_r} + \frac{1}{C_e}\right)_{v(\mathbf{r})}$$

$$\approx A(N_n) + d(N_{n,r} + N_{n,e})\left(\frac{\partial A}{\partial N_n}\right)_{v(\mathbf{r})} + \left(\frac{dN_{n,r}^2}{2C_r} + \frac{dN_{n,e}^2}{2C_e}\right)_{v(\mathbf{r})} = A(N_n)_{cap,parallel}, \quad (18)$$

where the mixed $2N_eN_r$ term has been neglected and the charges have been assigned to individual capacitors. The parallel capacitor schemes were developed and used in Refs. 38 and 17, but the aforementioned systematic expansion shows that various terms are neglected in the multicapacitor schemes for mathematical convenience without physical reasoning.

The previous equation also highlights the emergence of two different effective capacitances if the mixed terms are neglected and if charges are assigned to individual capacitors. These extrathermodynamic assumptions are due to system partitioning and have been shown to lead to unphysical behavior of reaction energies when a multicapacitor scheme is combined explicit/implicit solvent models.[17] The previous equation also shows that current multicapacitor models cannot reliably distinguish between serial and parallel capacitors because both versions of Eq. (18) are equally suitable for fitting the Helmholtz energy even though the physical/chemical processes behind these equivalent circuits (or fits) are clearly distinct.

A slightly more robust partitioned capacitor approximation can be derived by inserting a parallel capacitance relation directly in Eq. (17),

$$A(N_n)_{cap,parallel} \approx A(N_n) + d(N_{n,r} + N_{n,e})\left(\frac{\partial A}{\partial N_n}\right)_{v(\mathbf{r})} + \frac{d(N_{n,r} + N_{n,e})^2}{2}\left(\frac{1}{C_r + C_e}\right)_{v(\mathbf{r})}, \quad (19)$$

which requires further assumptions to be useful. To move forward, one can assume that $N_{n,r}$ is significantly larger than $N_{n,e}$ leading to

$$A(N_n)_{cap,parallel} \approx A(N_{n,r0}) + N_{n,r}\left(\frac{\partial A}{\partial N_n}\right)_{v(\mathbf{r})} + \frac{1}{2}\left(\frac{N_{n,r}^2}{C_e + C_r}\right)_{v(\mathbf{r})}, \quad (20)$$

which is unsatisfactory because it presents an unsystematic Taylor expansion. A slightly better approximation is achieved if one assumes that $N_{n,r}^2 \gg N_{n,e}^2$ in which case $N_{n,e}^2$ is neglected but the $N_{n,r}N_{n,e} > N_{n,e}^2$ term is retained. This gives

$$A(N_n)_{cap,part,mixed} \approx A(N_{n,r0}) + dN_{n,r}\tilde{\mu}_{N_{n0}} + \frac{dN_{n,r}^2 + dN_{n,r}dN_{n,e}}{C_{eff}}, \quad (21)$$

where C_{eff} corresponds to the effective capacitance accounting for both the e and r subsystems. The last formula is equal to the equation developed originally in Ref. 11 for the partitioned capacitance scheme, containing the mixed $N_{n,r}N_{n,e}$ term. However, the origin of the mixed term was not discussed in the original reference and its appearance with the N_e^2 is difficult to justify from the Taylor expansion perspective alone. Inclusion of $N_{n,r}N_{n,e}$ without N_e^2 is mathematically valid only for $N_e \to 0$, i.e., when charge

30 June 2023 07:06:11

Published under an exclusive license by AIP Publishing

transfer is negligible or when electrostatic interactions through dipole/polarization effects dominate.

Another partitioned capacitance approximation is obtained by considering the differential form of Eq. (17). This will lead to the "average number of electrons" approach introduced in Ref. 17,

$$dA(N_r)_{cap,part,average} \approx \left(\tilde{\mu}_{N_{n0}} + \frac{d(N_{n,r} + N_{n,e})/2}{C_{eff}}\right) d(N_r + N_e), \quad (22)$$

which is closely related to Eq. (17), but the origin of denominator 2 is difficult to see as it does not appear in the differential form of the capacitance approximation [see Eq. (16)].

E. Dipole field approximations

Further approximations to the partitioned and multi-capacitor schemes are obtained through various electrostatic expansions.[11,18,42] The most systematic development in an electrocatalytic setup[11] starts from Eq. (21), the differential form of the mixed capacitor scheme,

$$\begin{aligned} dA(N_n)_{cap,part,mixed} &\approx \left(\tilde{\mu}_{N_{n0}} + \frac{2dN_{n,r} + dN_{n,e}}{C_{eff}}\right) dN_{n,r} \\ &= dA_{charge,field}. \end{aligned} \quad (23)$$

If the reactant charge variations are small compared to these of the electrode, $dN_{n,r} \ll dN_{n,e}$, and $dN_{n,e}/C_{eff}$ measures the electrode potential variation as a function of surface charge $N_{n,e}$. Then, one can write

$$\begin{aligned} dA(N_n)_{charge,field} &\approx [\tilde{\mu}_{N_{n0}} + dN_{n,e}/C_{eff}]dN_{n,r} \\ &= \tilde{\mu}(N_{n0} + dN_{n,e})dN_{n,r}. \end{aligned} \quad (24)$$

The electrochemical potential can be further separated to the standard state and electric potential contributions using Eq. (4). Neglecting the irrelevant standard state chemical potential leads to

$$dA(N_n)_{charge,field} \approx -\phi^E(\mathbf{r}, N_{n0} + N_{n,e})dN_{n,r}, \quad (25)$$

where it is indicated that the electric field depends on the surface charge $N_{n,e}$. It should be noted that the above-mentioned interaction is strictly electrostatic and the spatial extent of $\phi_e(\mathbf{r})$ should depend on the electrolyte and the approach used to divide the total charge density to the electrode and reactant subsystems. The electrostatic potential created by the electrode can be computed from the Coulomb equation

$$\phi^E(\mathbf{r}) = \int d\mathbf{r}' \frac{\rho^E(\mathbf{r}')}{|\mathbf{r} - \mathbf{r}'|}, \quad (26)$$

where $\rho^E(\mathbf{r}')$ is the electrode charge density. In the above-mentioned equation and throughout the work, we use atomic units where the vacuum permittivity term, $4\varepsilon_0 = 1$, is absent from the denominator of Eq. (26). For this reason, the permittivity does not appear in the following equations. If Eq. (26) is applied to continuum solutions, the solvent permittivity should be included in it and all equations derived from it. Furthermore, it should also be noted that $\rho^E(\mathbf{r}')$ cannot be uniquely defined since charge partitioning cannot be achieved without approximations, and $\phi^E(\mathbf{r})$ should be considered as an effective quantity. Nevertheless, the electrostatic interaction (free) energy between e and r is defined as[43]

$$A_{es} = \int d\mathbf{r}' \frac{\phi^E(\mathbf{r})\rho^r(\mathbf{r})}{|\mathbf{r} - \mathbf{r}'|}, \quad (27)$$

where $\rho^r(\mathbf{r})$ is the charge density of the reactant. The full electrostatic interaction is expressed through a multipole expansion,[43]

$$A_{es} \approx q^E q^r + \frac{1}{2}\vec{\mathscr{E}}^E(\mathbf{r})M^r + \frac{1}{3}\frac{\partial\vec{\mathscr{E}}^E(\mathbf{r})}{\partial\mathbf{r}}\overleftrightarrow{\alpha}^r + \cdots, \quad (28)$$

where q^E is the electrode (surface) charge, q^r is the reactant charge, $\vec{\mathscr{E}}^E$ is the electric field generated by the electrode, M^r is the reactant dipole moment, $\frac{\partial\vec{\mathscr{E}}^E(\mathbf{r})}{\partial\mathbf{r}}$ is the electric field gradient, and $\overleftrightarrow{\alpha}^r$ is the quadrupole tensor of r. It should be noted that the multipole expansion is known to diverge when the distance between the electrostatic potential (ϕ^E) and charge distribution (ρ^r) is smaller than the radius within which the expansion is carried out:[43] when the electrode and reactant regions overlap, the electrostatic interaction energy is ill-defined. It is, therefore, questionable whether the expansion is valid when applied to potential/charge-dependent adsorption energies, a typical application of the dipole field approximation, where the molecule and electrode are spatially very close to each other.[11,18,42] We shall return to this issue in Sec. II H.

Nonetheless, the differential electrostatic interaction energy can be defined as

$$\begin{aligned} dA_{es} \approx{}& dq^E + dq^r + \frac{1}{2}\left(\vec{\mathscr{E}}^E(\mathbf{r})dM^r + M^r d\vec{\mathscr{E}}^E(\mathbf{r})\right) \\ &+ \frac{1}{3}\left(\frac{\partial\vec{\mathscr{E}}^E(\mathbf{r})}{\partial\mathbf{r}}d\overleftrightarrow{\alpha}^r + \overleftrightarrow{\alpha}d\left[\frac{\partial\vec{\mathscr{E}}^E(\mathbf{r})}{\partial\mathbf{r}}\right]\right) + \cdots, \end{aligned} \quad (29)$$

where $dq^E + dq^r = 0$ due to charge conservation in the canonical ensemble—for a real electrochemical interface or the GCE, there is no need for such a condition. While the previous equation can be used to write the electrostatic energy as a function of the field [see Eq. (32)], in the dipole field approximation only $M^r d\vec{\mathscr{E}}^E(\mathbf{r})$ is typically included.[11,18,42] This choice assumes that changes in the reactant geometry do not impact the dipole moment and that the quadrupole can be neglected even for linear molecules, such as CO_2, which do not even have a permanent dipole.

A more general dipole field model can be constructed by accounting for non-linear field-dependencies, which are expected to be important for non-polar molecules and at high-electric fields present at electrochemical interfaces. These terms are included in the induced dipole moment (M^r_{ind}), and the total dipole moment is

$$M^r(\vec{\mathscr{E}}) = M^r_0 + M^r_{ind}(\vec{\mathscr{E}}^E) \approx M^r_0 + \alpha\vec{\mathscr{E}} + \beta\vec{\mathscr{E}}^2 + \cdots, \quad (30)$$

where M^r_0, α, and β are the intrinsic dipole moment, polarizability, and hyperpolarizability, respectively. A similar expansion could also be made to the quadrupole and higher moments. Including the

30 June 2023 07:06:11

Published under an exclusive license by AIP Publishing

induced dipole moment in the dipole field model of Eq. (28) results in

$$A_{dip-field}(\vec{\mathscr{E}^E}) \approx q^E q^r + \frac{\vec{\mathscr{E}^E}}{2}\left(M_0^r + \alpha\vec{\mathscr{E}^E} + \beta\vec{\mathscr{E}^{E2}} + \cdots\right), \tag{31}$$

which is the field-dependent model used in, e.g., Ref. 19, to fit free energies as a function of the field. If the field is taken as an independent variable, we can write the differential dipole field free energy as

$$dA_{dip-field}(\vec{\mathscr{E}^E}) \approx \frac{d\vec{\mathscr{E}^E}}{2}\left(M_0^r + \alpha\vec{\mathscr{E}^E} + \cdots\right), \tag{32}$$

which assumes that the polarizability does not depend on the field strength and that field gradients can be omitted. While these may be reasonable assumptions at least for flat surfaces, their validity should be demonstrated, e.g., for stepped surfaces or nanostructures such as particles or dentrites.[24]

In practice, the effective dipole field differential free energy is often estimated as[11,18,24,42]

$$\begin{aligned} dA_{eff.dip-field} &\approx M_{eff}^r \times d\mathscr{E}_{eff}(\Delta U(N_e^{eff})) \\ &= M_{eff}^r C_{eff} dU(N_e^{eff}) \\ &= M_{eff}^r dN_n, \end{aligned} \tag{33}$$

where "*eff*" denotes effective. This effective dipole field model can be interpreted as an effective dipole interacting with the effective field obtained by assuming an effective interfacial capacitance of the electrochemical interface at an effective surface charge. We consider $d\mathscr{E}_{eff}$ an effective electric field because it is not really evaluated or utilized in actual applications of the dipole field models.[14,24,42] Rather, $d\mathscr{E}_{eff}$ serves the purpose of justifying the use of the dipole field interaction as the underlying mechanism for potential or charge-dependent adsorption energetics. Overall, the large number of effective quantities prevents detailed understanding of which interactions really contribute to the fitted dipole field model.

The dipole field model in its different forms has mostly been applied to simulate adsorption energies of linear molecules that do not have an intrinsic dipole moment, such as CO_2. Hence, the dominant contribution in the dipole field model would be the polarizability term, which is in the meV range and much smaller than the field dependencies computed in the literature.[11,18,24,42] To deal with this issue, the dipole field models typically use an *effective surface dipole* moment[11,18,24,42]—a property of the entire interface with an adsorbate rather than the reactant alone. Often, the surface dipole is treated as an effective quantity for fitting dA as a function of the total charge or the explicit electric field. Since the field is related to the surface charge by Gauss's law, the slope of A_{es} as a function of the surface charge gives an estimate for M^r.[11] While fitting A_{es} works very well in practice,[11,42] it remains unclear whether this fit captures *only* the dipole field interactions or whether other interactions also contribute to the slope. For instance, the effective (surface) dipole moment M_{eff}^r is considered constant even though it should depend on the field [Eq. (32)].

In addition to fitting the effective dipole moment, it can also be extracted using the work function changes due to adsorption in the canonical ensemble.[14,24,44,45] The effective dipole moment should then be viewed as a property of the entire surface + adsorbate system and the adsorbate must be considered as part of the surface.[24] While practical, combining the dipole field model with the effective surface dipole concept leads to a physically ambiguous situation: the dipole field model describes the interaction energy between an effective dipole of the interface and the effective field generated by the very same interface. In this situation, the dipole field model should break down since the underlying electrostatic multipole expansion [Eq. (27)] is not well-defined because the electrode and reactant can no longer be treated separately.

The aforementioned conceptual problem can be partially alleviated by treating the field as an external variable, as shown in Eq. (31), which develops the dipole field model from a Taylor expansion of the canonical free energy with respect to the electric field[19] rather than the multipole expansion. To achieve the Taylor expansion rigorously, the free energy should be written as a functional of the electric field ($A[\mathscr{E}^E]$) However, the connection between $A[\mathscr{E}^E]$ and Helmholtz or grand free energies is not straightforward because these are not functionals of the electric field, but rather, functions of the number of particles and chemical potentials, respectively. Unlike the number of electrons or electrode potential, the electric field depends on properties of the electrolyte and is not a suitable independent thermodynamic variable for electrochemical interfaces. Furthermore, while an external electric field can easily be added to standard DFT calculations, connecting the external field to the applied electrode potential cannot be achieved without free parameters.[46] A third way to arrive at the dipole field model is the electrostatic conceptual DFT approach treated as follows in Eq. (34).

F. Impact of geometric changes

Up to this point, we have focused solely on the $\partial A/\partial N dN$ terms, and the second term in Eq. (6) related to variations in the external (nuclear) potential has been ignored. Explicit treatment of this contribution is mostly missing from the capacitor-like models in the literature but should be included in general. Without compromising generality, the nuclear potential ($\delta v(\mathbf{r})$) can be assumed to present changes in the external nuclear potential brought about by geometric changes.

A notable exception is the recent dipole- or force-dependent method, which we call the dipole-force model,[12] developed to estimate electrode potential effects on transition state energy with canonical DFT calculations. This method implicitly includes geometry-dependency in both potential and geometric variables (R) through the reactant or surface dipole moment along the reaction coordinate $\vec{\omega}$: $dA_{dip-force}(R,U) \approx U \times \frac{\partial \vec{M}}{\partial R} \cdot \vec{\omega}$ for a macroscopically large electrode.[12] This clever scheme was shown to work well for "short" reaction pathways, when the reaction coordinate can be taken as a single bond length, and when the dipole-field and capacitor-based approximations hold. However, the method cannot be used when the reactant or solvent structures/geometries change drastically as a function of the electrode potential or when the reaction coordinate depends on the electrode potential. Difficulties for such systems likely result from the capacitor approximation focusing only on the effective dipole moment rather than the dipole vector, and the difficulty of determining the reaction coordinate for complex reactions.

30 June 2023 07:06:11

Published under an exclusive license by AIP Publishing

We next show how this dipole-force model can be related to the general geometric term through electrostatic conceptual DFT.[47,48] One first realizes that the $\int \left(\frac{\delta A}{\delta \nu(\mathbf{r})}\right)_{\{N_i\}} \delta\nu(\mathbf{r})d\mathbf{r}$ term can be simplified by writing $\left(\frac{\delta A}{\delta \nu(\mathbf{r})}\right)_{\{N_i\}} = \rho(\mathbf{r})$.[28] In its original formulation, electrostatic DFT describes only the electrostatic energy in terms for the *electronic* dipole moment.[47,48] To describe the electrostatic energy using the *total* dipole moment, we need to account for nuclear degrees of freedom and the nuclear dipole moment. This can be achieved within the multicomponent conceptual DFT framework, as shown in the supplementary material. Within the electrostatic conceptual DFT approximation, the first-order geometric term is

$$dA_{dip-geom} \approx d\vec{\mathscr{E}} \cdot \vec{M}, \tag{34}$$

indicating that $A_{dip-geom} \approx \vec{\mathscr{E}} \cdot \vec{M}$ and the total differential $dA_{dip-geom} \approx d\vec{\mathscr{E}} \cdot \vec{M} + d\vec{M} \cdot \vec{\mathscr{E}}$. Here, changes in both the field and dipole moment are considered, and the model presents a generalization of the dipole-field method developed in Ref. 12. Our derivation also presents an alternative way to obtain the dipole-field model without a multipole expansion, but an external electric field has to be assumed.

The relation between the external field and electrode potential can be sought through Gauss' theorem similar to Eq. (33). Keeping the field constant and assuming it mimics the electrode potential, $dA_{dip-geom}$ is a model for the energetics of electrode potential-driven changes in the geometry. Considering geometric changes only along the reaction coordinate leads to a conceptual DFT equivalent of the dipole-force model,

$$dA_{dip-geom}(\vec{\omega}) \approx U \times (d\vec{M} \cdot \vec{\omega}), \tag{35}$$

which shows that the dipole-force method[12] can be seen as the first-degree approximation to the geometric term of the electrostatic conceptual DFT. This development also reveals another side of dipole-force and dipole-field methods—they can also be derived using electrostatic conceptual DFT rather than pure electrostatics. As shown in Sec. II G and discussed in Sec. II G, switching to the conceptual DFT framework allows us to include other interactions and corrections in addition to electrostatics.

G. Separating chemical and electrostatic interactions

The above-mentioned analysis on different electrostatic corrections has relied on the assumption that chemical and electrostatic contributions can be separated or differentiated. But are these valid assumptions? This question dates back to the first electrostatic correction, the Frumkin model, which was developed originally for outer-sphere reactions.[26,49] The appropriateness of the Frumkin model for outer-sphere electrochemical electron transfer was recently verified for graphene-modified electrodes[50] through meticulous experiments and an extension of the Schmickler–Newns–Anderson model Hamiltonian[51,52] to include a Frumkin-like correction term.[50] However, it has been argued that the Frumkin or other electrostatic corrections cannot distinguish between specific adsorption and local electrostatic effects.[26] This view is also supported by our analysis and, in particular, Eq. (18) shows that the same energy expression can be derived for two different equivalent circuits. As shown in Fig. 2, different circuits present different physical and chemical processes indicating that the capacitor models cannot distinguish between double-layer charging, charge-transfer reactions, or adsorption processes.

These observations indicate that the distinction between electrostatics and chemical interactions is at least somewhat artificial and that electrostatic corrections can be cast as covalent chemical interactions and vice versa. This bears direct relevance not only for fundamental electrochemistry but also electrocatalyst design. For instance, it has been suggested that dipole-field interactions are important for single-atom catalysts in CO_2 reduction[11,14,42] but the many approximations in the dipole-field model itself makes it difficult to assess this suggestion. On the other hand, potential-dependency of CO_2 adsorption can be equally approached using, e.g., a classical donation–backdonation method[53] or charge-transfer interactions[54] addressed with, e.g., conceptual DFT.

To test the separation of electrostatic and charge-transfer interactions, we develop a conceptual DFT model for a simple electrosorption step with charge transfer. We follow the conceptual DFT reactivity approach[54] applied successfully to, e.g., ion-pair formation[55] and charge-transfer interactions,[54] but extend the model to an electrochemical interface. This model describes the influence of charge transfer on the reaction energy of a generic electrochemical reaction $A + B \rightarrow AB$ (where A is the adsorbate, B is the electrode, and AB is the chemisorbed state) as

$$\Delta E_{AB} = \left(\tilde{\mu}_B^0 - \tilde{\mu}_A^0\right)\Delta N + \frac{1}{2}\left(\eta_B^0 + \eta_A^0\right)\Delta N^2, \tag{36}$$

where ΔN denotes the charge transfer between A and B during the reaction, while the superscript "^{0}" denotes quantities computed at the chosen reference state. The first term includes the reference electrode potential and molecule chemical potential, which is directly related to its redox properties through its ionization energy and electron affinity.[56] The second term is chemical hardness, $\eta_i = \left(\frac{\partial^2 E_i}{\partial N_i^2}\right)_{\nu(\mathbf{r})} = \left(\frac{\partial \tilde{\mu}_i}{\partial N_i}\right)_{\nu(\mathbf{r})}$. For electrochemical interfaces, the hardness is related to the effective electrode capacitance through Eq. (8): $\eta_B = \frac{1}{C_{eff}^B}$. For molecule A, the hardness depends on its redox properties such as electron affinity and ionization potential.[56] Hence, Eq. (36) can be seen as a correction to electrosorption energies due to charge transfer between A and B.

As shown in the supplementary material, the differential adsorption energy as a function of the electrode potential ($\tilde{\mu}_B$) is

$$d\Delta E_{AB}(\tilde{\mu}_B) \approx \delta N\left[\tilde{\mu}_B^0 - \tilde{\mu}_A^0 + \Delta N_0 \times \left(\eta_A^0 + \eta_B^0 + \frac{1}{\delta N}\right)\right]d\tilde{\mu}_B, \tag{37}$$

where ΔN_0 is the charge transfer between A and B at a reference potential and δN denotes the potential-dependent change from ΔN_0. As discussed in detail in the supplementary material, Sec. S4.1, $d\Delta E_{AB}(\tilde{\mu}_B)$ depends on changes in both the adsorbate charge and electrode potential. Hence, $\left[\tilde{\mu}_B^0 - \tilde{\mu}_A^0 + \Delta N_0 \times \left(\eta_A^0 + \eta_B^0 + \frac{1}{\delta N}\right)\right]$ acts as the kernel, which determines how the potential-dependent changes in the adsorbate charge impact the adsorption energy.

30 June 2023 07:06:11

Published under an exclusive license by AIP Publishing

The previous equation has the same form as the dipole-field model [Eq. (33)] and can equally well be used for fitting potential-dependent adsorption energies. However, the conceptual and physical insights from these models are very different: the dipole-field model interprets the slope as a dipole moment, while the slope of Eq. (37) measures how the reaction energy depends on charge transfer as a function of the electrode potential. Accordingly, the dipole-field model would predict that electrostatics, interfacial dipoles, and electric fields are the key quantities in electrocatalysis, whereas the model based on the conceptual DFT emphasizes the importance of charge transfer and (electro)chemical potential equalization. This notion is strengthened by observing that the previous equation provides a conceptual DFT-based route to the recent model developed by Ringe[23] to quantify charge transfer and potential of zero-charge effects in electrocatalysis.[57]

H. Testing the models for electroadsorption: Electrostatics, charge transfer, or covalent bonding

While electrostatic and charge transfer contributions cannot, in general, be separated for weak interactions,[58] it remains an open question whether the separation is possible for a strong chemisorption bond. To answer this question, we consider the CO_2 adsorption on an iron–nitrogen–graphene single-atom catalyst, Fe–NC. We first computed grand-canonical adsorption free energies and subsequently fitted different electrostatic models to these energies in order to assess how well these approximations reproduce the explicitly potential-dependent adsorption energies. In addition to fitting adsorption energies, our goal is to analyze whether the interaction between Fe–NC and CO_2 can be *understood* within the dipole-field model, the charge transfer approach, or if something more complex is needed. The studied system is motivated by the proven success of dipole-field and capacitor models to fit the adsorption energy as a function of the electrode potential and surface charge for single-atom electrocatalysts.

Adsorption energies as a function of the electrode potential are given in Table II. Between −1.0 and −0.25 V, the adsorption energy changes linearly as a function of the electrode potential. When the potential is between −0.25 and 0.0 V, the surface charge changes from negative to positive. Below 0.0 V, CO_2 adsorbs on the surface, but above this potential, CO_2 spontaneously desorbs from the surface upon structural optimization. This behavior is in quantitative disagreement with the capacitor approximation, which predicts that (differential) adsorption energy is symmetric with respect to the potential of zero charge (see Fig. S1).

Consequently, we evaluated the effective capacitance by fitting the adsorption energies using different capacitor models. The results in Table III show that the computed capacitances of the same surface depend sensitively on the chosen model as they vary between 2.7 and 24 $\mu F/cm^2$. The smallest capacitance difference is that of the pristine Fe–NC and CO_2 adsorbed on Fe–NC computed from the direct definition of effective capacitance [Eq. (8)]. Extracting C_{eff} from the adsorption energies within the original capacitor model [Eq. (16)] leads to a significantly smaller capacitance. The partitioned capacitor model of Eq. (18), on the other hand, gives a much larger capacitance for the surface but the value is in line with the capacitance of pristine graphene.[59] Other partitioned capacitor models were not considered because they assume that the adsorbate charge should remain unaltered, but Table IV clearly shows that the CO_2 charge does not remain constant—hence the assumption $N^2_{n,r} \gg N^2_{n,e}$ leading to the mixed capacitor does not hold.

The dipole-field model achieves a good qualitative agreement between the electrode charge or potential and adsorption energy. As a linear dependency between charge and adsorption energy is seen, the effective dipole moment can be obtained from Eq. (33), which gives 0.59 e Å or 2.83 Debye at −0.5 V in good agreement with the corresponding values in Ref. 11. However, the dipole moment from the dipole-field model is surprisingly large—almost five times the gas-phase dipole moment of fully reduced CO_2^-, which is 0.55 Debye. Table IV shows that the adsorbed CO_2 carries a significant negative charge but the fitted dipole moment of 2.81 Debye cannot arise from the CO_2 alone. It might be possible that this large dipole moment effectively implies stronger stabilization of the system due to its interaction with the electric field.[14] Such a large dipole moment may also arise from the failure of the multipole expansion to dissect the adsorption interaction in dipole and field contributions as discussed in Sec. II E.

To analyze the results from the dipole-field model, the effective dipole moment was calculated from atomic charges. Assuming that CO_2–FeNC can be approximated as a diatomic molecule, the effective dipole moment is computed as

TABLE II. Analysis of CO_2 adsorption on Fe–NC as a function of the electrode potential. *U*: applied potential, Ω_{ads}: adsorption energies, *Mm*: magnetic moment, and *Q*: system charge of CO_2 + FeNC.

U/V	Ω_{ads}/eV	Mm	Q/e
0.0	−0.67	1.33	−0.48
−0.25	−1.03	1.13	−0.95
−0.5	−1.16	1.15	−1.22
−0.75	−1.32	1.06	−1.43
−1.0	−1.55	0.73	−1.77

TABLE III. Capacitance values extracted by fitting the GCE adsorption energies with different electrostatic models. C^{e+r}_{eff} is computed for the electrode + reactant system from GCE energies Eq. (8). C^{e+r}_{cap}, C^{e}_{cap}, and C^{r}_{cap} are the capacitance of the electrode + reactant and electrode systems from Eq. (16). C^{e}_{part} and C^{r}_{part} are for the partitioned capacitance model from Eq. (18). The unit is $\mu F/cm^2$.

C^{e+r}_{eff}	C^{e+r}_{cap}	C^{e}_{cap}	C^{e}_{part}	C^{r}_{part}
2.76	12.47	11.09	24.30	7.27

TABLE IV. Bader charges of CO_2 and Fe, and the dipole moment in both eÅ and Debye units calculated using Eq. (38) as a function of the applied potential *U*.

U/V	CO_2/e	Fe/e	eÅ	D
0.0	−0.66	1.73	2.39	11.48
−0.25	−0.74	0.26	1.00	4.80
−0.5	−0.77	−0.18	0.59	2.83
−0.75	−0.80	−0.42	0.38	1.82
−1.0	−0.85	−0.92	−0.07	−0.34

30 June 2023 07:06:11

Published under an exclusive license by AIP Publishing

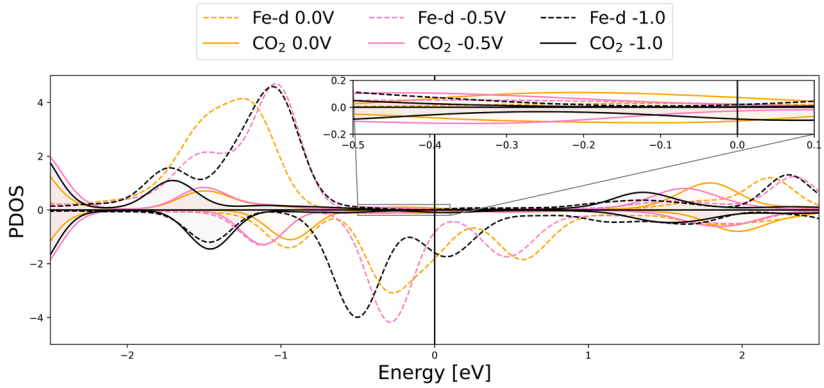

FIG. 3. The projected density of states for CO_2 adsorbed on Fe–NC as a function of the potential. The dashed lines indicate the iron d-states and the solid lines represent the CO_2 sp-states. The inset shows the states around the Fermi level. Electrode potentials are given on the standard hydrogen electrode (SHE) scale.

$$M_{eff} \approx \sum_i q_i(\mathbf{r}_i - \mathbf{r}_{cb}), \tag{38}$$

where $\mathbf{r}_i$ is the position of the ith nucleus and $\mathbf{r}_{cb}$ denotes the midpoint of the Fe–C bond. The potential-dependent dipole moments are given in Table IV and it is clearly visible that M_{eff} exhibits significant variations as a function of the electrode potential. The largest value is 16 times larger than the CO_2^- dipole moment and the smallest has a reversed direction, i.e., the dipole moment points from CO_2 to Fe. These features can be understood by the strong dependency between atomic charges and the electrode potential as shown in Table IV.

The above-mentioned analysis shows that adsorption energies can be fitted using capacitance and dipole-field approximations, but the physical insight depends on the chosen method and the computed capacitances or dipole moments do not always appear physically correct. To understand the source of these uncertainties, we performed a detailed analysis of CO_2 adsorption on Fe–NC as a function of the potential. First, it needs to be noted that separating the adsorption process into well-defined interactions is not straightforward. While atomic charges as a function of the potential can be easily computed, separating charge-transfer from electronic polarization, which is an electrostatic effect rather than charge-transfer, is difficult because charge partitioning cannot distinguish between these two effects. For an electronically adiabatic process, a more practical and somewhat more robust alternative to distinguish among charge-transfer, covalent bonds, and electrostatics is tracing the changes in the projected density of states (PDOS) upon adsorption as a function of the electrode potential.[60]

The PDOS $\rho(\varepsilon)(U) = \sum_i \left|\langle\Psi(\varepsilon';U)|\psi\rangle\right|^2 \delta(\varepsilon - \varepsilon')$, shown in Fig. 3, provides a quantitative and qualitative measure of the covalent interactions between adsorbate orbitals ($|\psi\rangle$) with the total wave function ($|\Psi\rangle$), and how this interaction changes as a function of the electrode potential U. The comparison of PDOS plots in Fig. 3 and Fig. S3 in the supplementary material shows that the covalent interactions between Fe and CO_2 take place mainly between −2.5 and 2.5 eV around the Fermi level. The PDOS plots show that there are only few CO_2 states around the Fermi level at all potentials. The bonding and antibonding states are located around −1.5–−1.0 eV and 1.5–2.0 eV depending on the potential. These figures also show that the covalent interactions depend very sensitively on the electrode potential and spin. At 0.0 V vs SHE (orange lines), there is a broad peak between −2 and −1 eV corresponding to filled CO_2 states. For the down-spin, a narrower peak for covalent interactions is observed at −1 eV. The iron down-spin states span the Fermi level while the up-spin has a band gap.

As the electrode potential is decreased, the surface becomes negatively charged and the PDOS goes through a series of notable changes. The filled Fe up-spin states are split, while the down-spin states move to lower energies as the potential is decreased from 0.0 to −0.5 V. As shown in Table II, the iron spin changes significantly. On the other hand, the CO_2 states remain rather unchanged. As the potential is further decreased to −1.0 V, the CO_2 and corresponding Fe states move to lower energies. The Fe down-spin states become more occupied and the Fe spin state approaches zero (Table II). At other potentials, similar changes are observed (Fig. S3).

The above-mentioned analysis shows that the CO_2 interaction with the Fe–NC catalyst is very complex. The adsorption energy is not only sensitive to the electrode potential but also notable changes in atomic charges point to charge-transfer effects, while the PDOS shows that the covalent bonding depends on both the potential and spin. As discussed, both the dipole-field and capacitor models can accurately fit potential-dependent adsorption energy. However, it is very questionable whether either model often used for CO_2 adsorption on Fe–NC-type materials can condense this complex chemistry to a single parameter.

III. DISCUSSION

This work systematically derives and discusses various electrostatic corrections that have been developed to study electrocatalytic thermodynamics and kinetics within canonical, constant charge DFT without explicitly treating the electrode potential. We have analyzed different electrostatic models in detail to understand the assumptions, limitations, and physical/chemical implications of the different electrostatic approximations. As it has been widely demonstrated in the literature that these methods can capture or fit potential-dependent reaction energies, our primary goal is to analyze what physicochemical insight can be obtained from the different electrostatic corrections to canonical DFT. We also propose

30 June 2023 07:06:11

Published under an exclusive license by AIP Publishing

some alternative approaches to extend canonical DFT to electrochemical systems. The present work answers the question as to which extent canonical DFT can approximate the in-principle exact thermodynamics from GCE-DFT.[61]

Through free energy differentiation, it was shown that the capacitor and dipole-field approximations only focus on changes in the number of particles, whereas geometric changes are usually ignored. This essentially means that the electrostatic corrections cannot account for the interplay between energetics, potential, and geometry. As such, these approaches cannot be applied to situations where the adsorption, transition state, or electrolyte configuration changes as a function of the electrode potential. While this might be a reasonable assumption for simple molecules, this can hardly be the case for complex molecules with different binding motifs and orientations.

A closely related issue pertains to the infinite-cell extrapolation schemes,[62,63] which are often used for validating or parametrizing electrostatic models. In particular, it is not always explicitly specified whether geometric variations are accounted for when the cell/charge extrapolation is performed. If the transition state and other geometries are not optimized at all different charge states and cell sizes, the situation schematically shown Fig. 4 arises. Specifically, without accounting for the geometric contribution, the extrapolation scheme is not a fully reliable reference. It is also questionable whether the extrapolation scheme can treat $\tilde{\mu}_n$ and $\tilde{\mu}_\pm$ as independent thermodynamic variables since the electrode potential ($\propto \tilde{\mu}_n$) is changed by including a different concentration of cations/anions ($\propto \tilde{\mu}_\pm$) in the simulation cell.

The main issue with the original capacitor model in the fully canonical situation [Eq. (14)] is the use of an effective capacitance that makes the model insensitive toward electrolyte properties. The electrolyte effects can, however, be included in the semi-grand canonical ensemble [Eq. (15)]. If the common approximation of effective capacitance is made, the electrode and electrolyte properties cannot be addressed separately, while this is possible both experimentally and in GCE-DFT calculations. The effective capacitor model cannot capture the subtle interplay between the electrode potential and charge, which is a fundamental feature of an electrochemical interface.

Another issue with the constant capacitance assumption is related to the description of electrode potential effects in reaction energies [Eq. (1)] when geometric changes take place. We have shown that for CO_2 adsorption on Fe–NC, and more generally for different initial and final states,[64] the effective capacitance is not constant. Furthermore, the capacitance should not be treated as a free variable to convert adsorption energies from canonical, constant charge calculations to potential-dependent adsorption energies as shown in the supplementary material, Sec. S2. The capacitor model also predicts the differential free energy to be symmetric and parabolic with respect to the PZC. This would indicate that both negative and positive applied potentials would lead to identical free energy changes as a function of the electrode potential, which is not observed in numerical GCE-DFT simulations. Despite these theoretical issues, the capacitor model seems robust, in practice, for metallic electrodes and when (potential-induced) changes in geometry are small. However, the effective capacitance should not be used as a free parameter but should be self-consistently computed for a given system using the chosen capacitor model. Finally, if the capacitance scheme is to be applied to semiconductor electrodes, space-charge capacitance should be included in C_{eff}.

The partitioned capacitance approaches include further approximations as partitioning is mathematically ambiguous because some terms in the free energy Taylor expansion are neglected and it is not *a priori* clear how these omissions impact different systems. The partitioned capacitance [Eq. (18)] will always suffer from artificial separation of the electrochemical interface to the electrode and reactants/double-layer subsystems, which makes the model prone to computational artifacts as noted in Ref. 17. This can lead to a situation where different parts of the system have seemingly different capacitances. This thermodynamic inconsistency is, however, a computational artifact resulting from system partitioning and/or the use of mixed explicit–implicit solvent models: the division into different subsystems cannot be done without extrathermodynamic assumptions.

Also, the physical interpretation of partitioned capacitance approaches is problematic because the total capacitance cannot be uniquely separated to double-layer, Helmholtz, or Gouy–Chapman charging and electrosorption (adsorption) contributions without extrathermodynamic assumptions. Based on an impedance spectroscopy perspective (Fig. 2) and Eq. (18), the Grahame model and parallel capacitors should be the most appropriate representations for adsorption and double-layer charging while the Gouy–Chapman–Stern model should be used for explicit/implicit double layers. In practice, however, Eq. (18) cannot separate between these two physically very distinct cases: by fitting $A(N_n)$ with Eq. (18), it is not possible to separate (1) DL charging and charge transfer due to adsorption or (2) separate explicit (Helmholtz) and implicit (DL) charging processes. Another partitioned parallel capacitor model, Eq. (21), is expected to perform better for electrosorption energies but only when charge transfer between

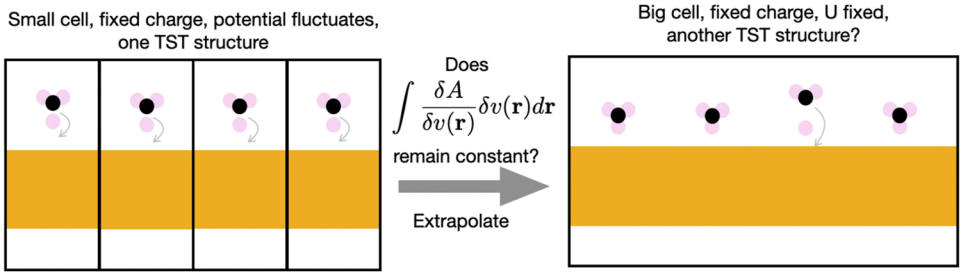

FIG. 4. The geometric term in cell-size extrapolation. If the TST is not recalculated for each cell size, the geometric term, $\int \frac{\delta A}{\delta v(\mathbf{r})} \delta v(\mathbf{r}) d\mathbf{r}$, is not correctly accounted for in the extrapolation scheme.

30 June 2023 07:06:11

Published under an exclusive license by AIP Publishing

the electrode and double-layer or reactant is negligible. The average capacitor model, Eq. (22), introduces least approximations and is, therefore, expected to be the most robust partitioned capacitor scheme. Finally, if the partitioned capacitors are used for semiconductor electrodes, the space-charge capacitance C_{eff} should also be included either in series or in parallel.

Even further approximations are introduced in the dipole-field model. While it was shown that this model can be derived by applying a multipole expansion on the partitioned capacitor model or through Taylor expansion with respect to the electric field, several theoretical issues were raised. First, the underlying partitioned capacitance model already contains several assumptions. Second, the multipole expansion is divergent when applied to spatially close interacting subsystems, such as those treated in chemisorption or electrosorption problems. Third, only the dipole-field term of the full multipole expansion is retained and effects such as induced dipole moments or polarizability are typically omitted. For comparison, in the context of oriented electric field catalysis, higher-order field dependencies are needed even for qualitative understanding of polarization and field effects,[65] and the linear dependency between field and reaction energies seems to be valid only for a very narrow range of fields.[66] Fourth, the practical dipole-field model [Eq. (33)] contains several effective quantities such as effective capacitance, surface charge, and the dipole moment, which are effectively treated as fitting quantities in most cases. Fifth, the physical interpretation Eq. (33) is that of surface dipole interacting with the effective field generated by the surface itself. In this case, the electrostatic energy and the multipole model leading to the dipole-field model are not well-defined as discussed in Sec. II E. Sixth, the Taylor expansion with respect to the electric field is problematic because neither the canonical nor grand canonical ensembles or free energies are functionals of the electric field and the electric field cannot be considered an independent thermodynamic variable of an electrochemical interface because it depends on the properties of the electrolyte. These features limit the applicability, generality, and physical insight of the dipole-field models. Furthermore, our derivations show that it is necessary to test and parameterize the model and its many effective quantities for each surface and reactant. In practice, we observed that the dipole moments extracted from the dipole-field model appear unreasonably large and show substantial potential dependencies (Table IV). While these are acceptable traits of an effective model and for fitting purposes, fundamental understanding on the role of the electric field, dipole moments, polarizability, etc., should be approached cautiously, given the amount of effective quantities and implicit assumptions in the model.

We also addressed the general plausibility of separating chemical and electrostatic contributions. In line with previous studies on the Frumkin model, we conclude that electrostatics and chemical interactions or covalent bonding cannot, in general, be differentiated by studying reaction or adsorption free energies as a function of charge N_n or electrode potential U. By means of analytic arguments on the capacitor model [Eq. (18)] and by contrasting the dipole-field model with a charge transfer model derived using conceptual DFT [Eq. (37)], we have shown that just by fitting $A(N_n)$ or $\Omega(\tilde{\mu}_n)$, one cannot differentiate between charge-transfer and electrostatic interactions. While both electrostatic and charge-transfer models are equally suitable for fitting purposes, their physical implications are clearly different, which is a very important point for computational electrocatalyst design; the interpretation of electrocatalytic thermodynamics or kinetics based on electrostatic or charge-transfer models leads to different conclusions on which interactions determine electrocatalytic performance. As such, depending on the selected model, different quantities can be chosen for optimization in electrocatalyst development. Here, insights and approaches from conceptual DFT might prove to be very helpful as it offers a rigorous way to describe chemical interactions through, e.g., chemical softness or Fukui functions in addition to electrostatic or geometric terms. In fact, a detailed analysis of electrostatics and geometrical changes at electrochemical interfaces conducted in Ref. 67 has shown that general, reliable estimates of electrochemical thermodynamics are achievable with conceptual DFT, but this requires the inclusion of several high-order terms. We, therefore, propose that addressing geometric, electrostatic, and chemical interactions within conceptual DFT quantities would be very beneficial for the next generation of approximate electrochemical DFT schemes.

We wish to re-emphasize that all approximations discussed in this work have been successfully applied to predict or fit electrochemical thermodynamics and kinetics for different systems. At the same time, it needs to be emphasized that different electrostatic schemes have been developed and used for distinct systems, and it is important that the correct scheme is selected and tested for a particular problem. This is clearly shown in our analysis of potential-dependent CO_2 adsorption on a Fe–NC catalyst where largely varying capacitances and dipole moments were obtained with different approximations. We also showed that conceptual DFT approaches can be used to derive alternative and possibly more general ways to include geometric and potential dependencies in the electrocatalytic DFT approximations. Finally, if one wishes to avoid these electrostatic or conceptual DFT approximations altogether, GCE-DFT should be the method of choice. While GCE-DFT is not often employed in large-scale (screening) studies, its computational cost is only ~30% more than that of canonical DFT and it can already be readily applied to complex multi-step reactions[68] and even molecular dynamic simulations.[31]

IV. CONCLUSIONS

We have provided a detailed and systematic derivation of different electrostatic approximations developed to estimate the impact of the electrode potential on reaction thermodynamics and kinetics within canonical DFT. This allowed us to reveal the implicit assumptions behind these approximations and their limitations and physical implications. We have shown that these approximations efficiently capture or fit the potential-dependency in reaction energetics, but care should be exercised when physical or chemical insight other than energetics is drawn from them. Also, the validity of the chosen approximation should be carefully considered separately for each system. More specifically, several aspects and limitations have been discussed in detail: (1) the constant effective capacitance precludes the study of electrolyte/solvent effects, (2) the physical picture of partitioned capacitance schemes is unclear and extrathermodynamic assumptions are made to achieve separation to subsystems, (3) the dipole-field models contain multiple effective quantities

30 June 2023 07:06:11

Published under an exclusive license by AIP Publishing

limiting their predictive power, (4) the interplay between geometrical changes and the electrode potential is often neglected, (5) distinguishing between electrostatic, charge transfer, and covalent interactions is difficult, and (6) the computed capacitances, dipole moments, and physical insight depend sensitively on the selected approximation. Careful consideration of these issues allowed us to analyze model accuracy and insight, to suggest when a given model should be chosen, and to propose alternative formulations based on conceptual DFT or GCE-DFT.

V. COMPUTATIONAL METHODS

We performed grand-canonical ensemble density functional (GCE-DFT) simulations using the Solvated Jellium Model (SJM) method[69] as implemented in GPAW.[70] The solvent was treated using the dielectric continuum model for water developed in Ref. 71 and the vdW radius for Fe was set to 2.0 Å. The electronic structure was calculated on a real-space grid with a spacing of 0.2 Å, and a (3 × 3 × 1) k-point sampling was used. The Bayesian error estimation functional with van der Waals correlation (BEEF–vdW)[72] was used to model the exchange-correlation effects. The reactions were simulated on a graphene layer constituting 3 hexagonal rings per four and a half (54 atoms) with an Fe atom encrusted right in the middle surrounded by four N atoms to each connection to the graphene and one CO_2 molecule adsorbed on top of the Fe atom. A vacuum of 15 Å thickness was applied on the slab along the z-direction to prevent interactions of the slab with its upper and lower periodic images. The carbon atoms from the graphene layer were kept fixed, while the remaining atoms were allowed to relax.

The CO_2^- dipole moment was computed with NWChem 7.0.[73] The B3LYP-D3[74] function with the aug-cc-pVDZ basis set[75] for both C and O coupled with an ultrafine integration grid following the recommendation for accurate dipole moment calculations.[76] Geometry optimization was performed before the dipole moment calculation.

SUPPLEMENTARY MATERIAL

See the supplementary material for Taylor expansions of the grand canonical and canonical free energies, adsorption Helmholtz free energy as a function of the electrode potential: impact of capacitance, including the nuclear dipole in the electrostatic conceptual DFT picture, derivation of the electrocatalytic electrochemical potential equilibrium model, and additional DOS figures.

ACKNOWLEDGMENTS

The authors acknowledge funding by the Academy of Finland (CompEL Project No. 338228). The authors thank Dmitry Morozov for helping with the dipole moment calculations for charged systems. The computer resources were provided by the CSC-IT Center for Science Ltd.

AUTHOR DECLARATIONS

Conflict of Interest

The authors have no conflicts to disclose.

Author Contributions

F.D.-F. carried out the calculations and contributed to the theoretical analysis. M.M.M. conceived the idea and developed most of the theoretical analysis. Both contributed to writing the manuscript.

Fabiola Domínguez-Flores: Data curation (lead); Formal analysis (supporting); Investigation (equal); Visualization (lead); Writing – review & editing (equal). **Marko M. Melande**: Conceptualization (lead); Formal analysis (lead); Funding acquisition (lead); Investigation (equal); Methodology (lead); Project administration (lead); Resources (lead); Supervision (lead); Writing – original draft (lead); Writing – review & editing (equal).

DATA AVAILABILITY

The data that support the findings of this study are available within the article and its supplementary material.

APPENDIX: SUMMARY OF THE APPROXIMATIONS

Summary of the various approximations derived in this work.

REFERENCES

[1] *Atomic-Scale Modelling of Electrochemical Systems*, edited by M. M. Melander, T. T. L. Laurila, and K. Laasonen (John Wiley & Sons Ltd., Chichester, 2022).
[2] A. Y. Lozovoi, A. Alavi, J. Kohanoff, and R. M. Lynden-Bell, "*Ab initio* simulation of charged slabs at constant chemical potential," J. Chem. Phys. **115**, 1661–1669 (2001).
[3] N. D. Mermin, "Thermal properties of the inhomogeneous electron gas," Phys. Rev. **137**, A1441–A1443 (1965).
[4] R. Sundararaman, W. A. Goddard, and T. A. Arias, "Grand canonical electronic density-functional theory: Algorithms and applications to electrochemistry," J. Chem. Phys. **146**, 114104 (2017).
[5] M. M. Melander, M. J. Kuisma, T. E. K. Christensen, and K. Honkala, "Grand-canonical approach to density functional theory of electrocatalytic systems: Thermodynamics of solid-liquid interfaces at constant ion and electrode potentials," J. Chem. Phys. **150**, 041706 (2019).
[6] M. M. Melander, "Grand canonical rate theory for electrochemical and electrocatalytic systems I: General formulation and proton-coupled electron transfer reactions," J. Electrochem. Soc. **167**, 116518 (2020).
[7] N. Bonnet, T. Morishita, O. Sugino, and M. Otani, "First-principles molecular dynamics at a constant electrode potential," Phys. Rev. Lett. **109**, 266101 (2012).
[8] W. Schmickler and E. Santos, "Desorption of hydrogen from graphene induced by charge injection," ChemElectroChem **9**, e202200511 (2022).
[9] M. M. Melander, "Grand canonical ensemble approach to electrochemical thermodynamics, kinetics, and model Hamiltonians," Curr. Opin. Electrochem. **29**, 100749 (2021).
[10] N. Abidi and S. N. Steinmann, "How are transition states modeled in heterogeneous electrocatalysis?," Curr. Opin. Electrochem. **33**, 100940 (2022).
[11] S. Vijay, W. Ju, S. Brückner, S.-C. Tsang, P. Strasser, and K. Chan, "Unified mechanistic understanding of CO_2 reduction to CO on transition metal and single atom catalysts," Nat. Catal. **4**, 1024–1031 (2021).
[12] S. Vijay, G. Kastlunger, J. A. Gauthier, A. Patel, and K. Chan, "Force-based method to determine the potential dependence in electrochemical barriers," J. Phys. Chem. Lett. **13**, 5719–5725 (2022).
[13] A. M. Patel, S. Vijay, G. Kastlunger, J. K. Nørskov, and K. Chan, "Generalizable trends in electrochemical protonation barriers," J. Phys. Chem. Lett. **12**, 5193–5200 (2021).

30 June 2023 07:06:11

Published under an exclusive license by AIP Publishing

[14]S. Vijay, J. A. Gauthier, H. H. Heenen, V. J. Bukas, H. H. Kristoffersen, and K. Chan, "Dipole-field interactions determine the CO_2 reduction activity of 2D Fe–N–C single-atom catalysts," ACS Catal. **10**, 7826–7835 (2020).
[15]S. R. Kelly, C. Kirk, K. Chan, and J. K. Nørskov, "Electric field effects in oxygen reduction kinetics: Rationalizing pH dependence at the Pt(111), Au(111), and Au(100) electrodes," J. Phys. Chem. C **124**, 14581–14591 (2020).
[16]S. Ringe, C. G. Morales-Guio, L. D. Chen, M. Fields, T. F. Jaramillo, C. Hahn, and K. Chan, "Double layer charging driven carbon dioxide adsorption limits the rate of electrochemical carbon dioxide reduction on gold," Nat. Commun. **11**, 33 (2020).
[17]J. A. Gauthier, C. F. Dickens, H. H. Heenen, S. Vijay, S. Ringe, and K. Chan, "Unified approach to implicit and explicit solvent simulations of electrochemical reaction energetics," J. Chem. Theory Comput. **15**, 6895–6906 (2019).
[18]S. Ringe, E. L. Clark, J. Resasco, A. Walton, B. Seger, A. T. Bell, and K. Chan, "Understanding cation effects in electrochemical CO_2 reduction," Energy Environ. Sci. **12**, 3001–3014 (2019).
[19]L. D. Chen, M. Urushihara, K. Chan, and J. K. Nørskov, "Electric field effects in electrochemical CO_2 reduction," ACS Catal. **6**, 7133–7139 (2016).
[20]K. Chan and J. K. Nørskov, "Potential dependence of electrochemical barriers from ab initio calculations," J. Phys. Chem. Lett. **7**, 1686–1690 (2016).
[21]K. Chan and J. K. Nørskov, "Electrochemical barriers made simple," J. Phys. Chem. Lett. **6**, 2663–2668 (2015).
[22]J. A. Gauthier, C. F. Dickens, S. Ringe, and K. Chan, "Practical considerations for continuum models applied to surface electrochemistry," ChemPhysChem **20**, 3074–3080 (2019).
[23]S. Ringe, "The importance of a charge transfer descriptor for the screening of electrocatalysts at the example of CO_2 reduction," ChemRxiv:10.26434/chemrxiv-2022-hvf9g (2022).
[24]S. D. Beinlich, N. G. Hörmann, and K. Reuter, "Field effects at protruding defect sites in electrocatalysis at metal electrodes?," ACS Catal. **12**, 6143–6148 (2022).
[25]N. G. Hörmann, N. Marzari, and K. Reuter, "Electrosorption at metal surfaces from first principles," Comput. Mater. **6**, 136 (2020).
[26]G. A. Tsirlina, O. A. Petrii, R. R. Nazmutdinov, and D. V. Glukhov, "Frumkin correction: Microscopic view," Russ. J. Electrochem. **38**, 132–140 (2002).
[27]S. Trasatti, "The "absolute" electrode potential—The end of the story," Electrochim. Acta **35**, 269–271 (1990).
[28]P. Geerlings, F. De Proft, and W. Langenaeker, "Conceptual density functional theory," Chem. Rev. **103**, 1793–1874 (2003).
[29]M. Franco-Pérez, P. W. Ayers, J. L. Gázquez, and A. Vela, "Thermodynamic responses of electronic systems," J. Chem. Phys. **147**, 094105 (2017).
[30]T. Binninger, "Piecewise nonlinearity and capacitance in the joint density functional theory of extended interfaces," Phys. Rev. B **103**, L161403 (2021).
[31]M. Melander, T. Wu, and K. Honkala, "Constant inner potential DFT for modelling electrochemical systems under constant potential and bias," ChemRxiv:10.26434/chemrxiv-2021-r621x-v3 (2023).
[32]C. G. Van de Walle and R. M. Martin, "Theoretical calculations of heterojunction discontinuities in the Si/Ge system," Phys. Rev. B **34**, 5621–5634 (1986).
[33]J. K. Nørskov, J. Rossmeisl, A. Logadottir, L. Lindqvist, J. R. Kitchin, T. Bligaard, and H. Jónsson, "Origin of the overpotential for Oxygen reduction at a fuel-cell cathode," J. Phys. Chem. B **108**, 17886–17892 (2004).
[34]D. Bruch, C. Balzer, and Z.-G. Wang, "Thermodynamics of electrolyte solutions near charged surfaces: Constant surface charge vs constant surface potential," J. Chem. Phys. **156**, 174704 (2022).
[35]D. Gunceler, K. Letchworth-Weaver, R. Sundararaman, K. A. Schwarz, and T. A. Arias, "The importance of nonlinear fluid response in joint density-functional theory studies of battery systems," Modell. Simul. Mater. Sci. Eng. **21**, 074005 (2013).
[36]J. Wu, "Understanding the electric double-layer structure, capacitance, and charging dynamics," Chem. Rev. **122**, 10821–10859 (2022).
[37]J. Huang, "Surface charging behaviors of electrocatalytic interfaces with partially charged chemisorbates," Curr. Opin. Electrochem. **33**, 100938 (2022).
[38]P. Hutchison, R. E. Warburton, A. V. Soudackov, and S. Hammes-Schiffer, "Multicapacitor approach to interfacial proton-coupled electron transfer thermodynamics at constant potential," J. Phys. Chem. C **125**, 21891–21901 (2021).
[39]O. Gharbi, M. T. T. Tran, B. Tribollet, M. Turmine, and V. Vivier, "Revisiting cyclic voltammetry and electrochemical impedance spectroscopy analysis for capacitance measurements," Electrochim. Acta **343**, 136109 (2020).
[40]J. Kang, J. Wen, S. H. Jayaram, A. Yu, and X. Wang, "Development of an equivalent circuit model for electrochemical double layer capacitors (EDLCs) with distinct electrolytes," Electrochim. Acta **115**, 587–598 (2014).
[41]J. Huang and C.-K. Li, "Impedance response of electrochemical interfaces: Part II-chemisorption," J. Phys.: Condens. Matter **33**, 164003 (2021).
[42]N. Karmodak, S. Vijay, G. Kastlunger, and K. Chan, "Computational screening of single and di-atom catalysts for electrochemical CO_2 reduction," ACS Catal. **12**, 4818–4824 (2022).
[43]A. Stone, *The Theory of Intermolecular Forces* (Oxford University Press, 2013).
[44]W. Schmickler, "The surface dipole moment of species adsorbed from a solution," J. Electroanal. Chem. Interfacial Electrochem. **249**, 25–33 (1988).
[45]Under electrochemical conditions or in GCE-DFT this practice would be inapplicable because the work function does not change because it is fixed by the electrode potential.
[46]D. Luan and J. Xiao, "Adaptive electric fields embedded electrochemical barrier calculations," J. Phys. Chem. Lett. **14**, 685–693 (2023).
[47]L. Komorowski, J. Lipiński, and P. Szarek, "Polarization justified Fukui functions," J. Chem. Phys. **131**, 124120 (2009).
[48]T. Clarys, T. Stuyver, F. De Proft, and P. Geerlings, "Extending conceptual DFT to include additional variables: Oriented external electric field," Phys. Chem. Chem. Phys. **23**, 990–1005 (2021).
[49]W. R. Fawcett, "Fifty years of studies of double layer effects in electrode kinetics—A personal view," J. Solid State Electrochem. **15**, 1347 (2011).
[50]D.-Q. Liu, M. Kang, D. Perry, C.-H. Chen, G. West, X. Xia, S. Chaudhuri, Z. P. L. Laker, N. R. Wilson, G. N. Meloni, M. M. Melander, R. J. Maurer, and P. R. Unwin, "Adiabatic versus non-adiabatic electron transfer at 2D electrode materials," Nat. Commun. **12**, 7110 (2021).
[51]W. Schmickler, "A theory of adiabatic electron-transfer reactions," J. Electroanal. Chem. Interfacial Electrochem. **204**, 31–43 (1986).
[52]J. Huang, P. Li, and S. Chen, "Quantitative understanding of the sluggish kinetics of hydrogen reactions in alkaline media based on a microscopic Hamiltonian model for the Volmer step," J. Phys. Chem. C **123**, 17325–17334 (2019).
[53]C. G. Vayenas and S. Brosda, "Electron donation–backdonation and the rules of catalytic promotion," Top. Catal. **57**, 1287–1301 (2014).
[54]R. A. Miranda-Quintana, P. W. Ayers, and F. Heidar-Zadeh, "Reactivity and charge transfer beyond the parabolic model: The "$|\Delta\mu|$ big is good" principle," ChemistrySelect **6**, 96–100 (2021).
[55]R. A. Miranda-Quintana and J. Smiatek, "Theoretical insights into specific ion effects and strong-weak acid-base rules for ions in solution: Deriving the law of matching solvent affinities from first principles," ChemPhysChem **21**, 2605–2617 (2020).
[56]R. A. Miranda-Quintana, M. Martínez González, and P. W. Ayers, "Electronegativity and redox reactions," Phys. Chem. Chem. Phys. **18**, 22235–22243 (2016).
[57]The potential-of-zero-charge effects are implicitly included in the reference state chosen for Eq. (37).
[58]T. Clark, "Polarization, donor–acceptor interactions, and covalent contributions in weak interactions: A clarification," J. Mol. Model. **23**, 297 (2017).
[59]J. Chen, C. Li, and G. Shi, "Graphene materials for electrochemical capacitors," J. Phys. Chem. Lett. **4**, 1244–1253 (2013).
[60]F. Dominguez-Flores, E. Santos, W. Schmickler, and F. Juarez, "Interaction between chloride ions mediated by carbon nanotubes: A chemical attraction," J. Solid State Electrochem. **24**, 3207 (2020).
[61]While some approximations, such as dielectric continuum solvent/electrolyte models, need to be used currently in practical GCE-DFT calculations, it should be noted that canonical DFT inherits all limitations of current GCE-DFT methods but many more are introduced when using canonical DFT and electrostatic corrections.
[62]E. Skúlason, V. Tripkovic, M. E. Björketun, S. Gudmundsdóttir, G. Karlberg, J. Rossmeisl, T. Bligaard, H. Jónsson, and J. K. Nørskov, "Modeling the electrochemical hydrogen oxidation and evolution reactions on the basis of density functional theory calculations," J. Phys. Chem. C **114**, 18182–18197 (2010).

30 June 2023 07:06:11

Published under an exclusive license by AIP Publishing

[63]J. Rossmeisl, E. Skúlason, M. E. Björketun, V. Tripkovic, and J. K. Nørskov, "Modeling the electrified solid–liquid interface," Chem. Phys. Lett. **466**, 68–71 (2008).
[64]M. D. Hossain, Y. Huang, T. H. Yu, W. A. Goddard III, and Z. Luo, "Reaction mechanism and kinetics for CO_2 reduction on nickel single atom catalysts from quantum mechanics," Nat. Commun. **11**, 2256 (2020).
[65]P. Besalú-Sala, M. Solà, J. M. Luis, and M. Torrent-Sucarrat, "Fast and simple evaluation of the catalysis and selectivity induced by external electric fields," ACS Catal. **11**, 14467–14479 (2021).
[66]N. M. Hoffmann, X. Wang, and T. C. Berkelbach, "Linear free energy relationships in electrostatic catalysis," ACS Catal. **12**, 8237–8241 (2022).
[67]J.-S. Filhol and M.-L. Doublet, "Conceptual surface electrochemistry and new redox descriptors," J. Phys. Chem. C **118**, 19023–19031 (2014).
[68]T. Wu, M. M. Melander, and K. Honkala, "Coadsorption of NRR and HER intermediates determines the performance of Ru-N_4 toward electrocatalytic N_2 reduction," ACS Catal. **12**, 2505–2512 (2022).
[69]G. Kastlunger, P. Lindgren, and A. A. Peterson, "Controlled-potential simulation of elementary electrochemical reactions: Proton discharge on metal surfaces," J. Phys. Chem. C **122**, 12771–12781 (2018).
[70]J. Enkovaara, C. Rostgaard, J. J. Mortensen, J. Chen, M. Dułak, L. Ferrighi, J. Gavnholt, C. Glinsvad, V. Haikola, H. A. Hansen, H. H. Kristoffersen, M. Kuisma, A. H. Larsen, L. Lehtovaara, M. Ljungberg, O. Lopez-Acevedo, P. G. Moses, J. Ojanen, T. Olsen, V. Petzold, N. A. Romero, J. Stausholm-Møller, M. Strange, G. A. Tritsaris, M. Vanin, M. Walter, B. Hammer, H. Häkkinen, G. K. H. Madsen, R. M. Nieminen, J. K. Nørskov, M. Puska, T. T. Rantala, J. Schiøtz, K. S. Thygesen, and K. W. Jacobsen, "Electronic structure calculations with GPAW: A real-space implementation of the projector augmented-wave method," J. Phys.: Condens. Matter **22**, 253202 (2010).
[71]A. Held and M. Walter, "Simplified continuum solvent model with a smooth cavity based on volumetric data," J. Chem. Phys. **141**, 174108 (2014).
[72]J. Wellendorff, K. T. Lundgaard, A. Møgelhøj, V. Petzold, D. D. Landis, J. K. Nørskov, T. Bligaard, and K. W. Jacobsen, "Density functionals for surface science: Exchange-correlation model development with Bayesian error estimation," Phys. Rev. B **85**, 235149 (2012).
[73]M. Valiev, E. J. Bylaska, N. Govind, K. Kowalski, T. P. Straatsma, H. J. J. Van Dam, D. Wang, J. Nieplocha, E. Apra, T. L. Windus, and W. A. de Jong, "NWChem: A comprehensive and scalable open-source solution for large scale molecular simulations," Comput. Phys. Commun. **181**, 1477–1489 (2010).
[74]S. Grimme, J. Antony, S. Ehrlich, and H. Krieg, "A consistent and accurate *ab initio* parametrization of density functional dispersion correction (DFT-D) for the 94 elements H-Pu," J. Chem. Phys. **132**, 154104 (2010).
[75]R. A. Kendall, T. H. Dunning, and R. J. Harrison, "Electron affinities of the first-row atoms revisited. systematic basis sets and wave functions," J. Chem. Phys. **96**, 6796–6806 (1992).
[76]J. C. Zapata and L. K. McKemmish, "Computation of dipole moments: A recommendation on the choice of the basis set and the level of theory," J. Phys. Chem. A **124**, 7538–7548 (2020).

30 June 2023 07:06:11

Published under an exclusive license by AIP Publishing